Ultrafast Spin Avalanches in Crystals of Nanomagnets in Terms of Magnetic Detonation

M. Modestov, V. Bychkov, and M. Marklund
Department of Physics, Umeå University, SE-901 87 Umeå, Sweden
(Received 19 May 2011; published 11 November 2011)

Recent experiments [W. Decelle *et al.*, Phys. Rev. Lett. **102**, 027203 (2009)] have discovered ultrafast propagation of spin avalanches in crystals of nanomagnets, which is 3 orders of magnitude faster than the traditionally studied magnetic deflagration. The new regime has been hypothetically identified as magnetic detonation. Here we demonstrate unequivocally the possibility of magnetic detonation in the crystals, as a front consisting of a leading shock and a zone of Zeeman energy release. We study the key features of the process and find that the magnetic detonation speed only slightly exceeds the sound speed in agreement with the experimental observations. For combustion science, our results provide a unique physical example of extremely weak detonation.

DOI: 10.1103/PhysRevLett.107.207208 PACS numbers: 75.50.Xx, 47.40.Rs, 47.70.Pq, 75.60.Jk

Molecular magnetism is a rapidly developing interdisciplinary research area within material science [1,2]. One of the widely investigated materials in the subject is Mn_{12} acetate, with a high spin number ($S = 10$) and strong magnetic anisotropy [1–5]. At sufficiently low temperature and for the magnetic field pointing along the easy axis, all the spins of the molecules occupy the ground state (e.g., $S_z = 10$ in Fig. 1); in this state the magnetization reaches its saturation value. When the magnetic field direction is switched to the opposite one, the former ground state becomes metastable with an increased potential energy (the Zeeman energy) and a barrier separating it from the new ground state. Active research on the subject has demonstrated that spin relaxation from the metastable to the ground state often happens in the form of a narrow front spreading in a sample with a velocity of a few meters per second [6–12]. Still, all these works focused on magnetic deflagration, i.e., a front of energy release propagating due to thermal conduction at velocities much smaller than the sound speed.

In contrast to other studies, recent experiments by Decelle *et al.* [13] encountered a new fast regime of the magnetic avalanches in Mn_{12} acetate with a front velocity exceeding the typical magnetic deflagration speed by 3 orders of magnitude. A small number of sensors in Ref. [13] led to large uncertainty in measuring the front velocity, which was, presumably, comparable to the sound speed ($c_0 \approx 2000$ m/s) in the crystals. Decelle *et al.* [13] suggested the hypothesis that the new regime was magnetic detonation. Reference [13] thus raised a number of important and nontrivial questions, requiring a large bulk of theoretical work to clarify the new phenomenon. For example, in contrast to the fast magnetic avalanches, combustion detonations demonstrate a front speed larger than the sound speed by an order of magnitude and a destructively high pressure [14].

In this Letter we resolve the most important issues raised by the experiments presented in Ref. [13]. We demonstrate unequivocally the possibility of magnetic detonation, in the form of a front with a leading shock and a zone of Zeeman energy release. We study the key features of the process and find that the magnetic detonation speed is only slightly greater than the sound speed, which is consistent with the experimental data [13]. Further experimental validation of our results requires a technique able to trace the instantaneous front position with better control of the avalanche ignition. Our results are also important for combustion science as they provide a unique physical example of extremely weak detonation.

In line with the experiments [13], we consider spin avalanches in Mn_{12} acetate with the Hamiltonian $\mathcal{H} = -\beta S_z^2 - g\mu_B H_z S_z$ suggested in [10]. Here S_z is the spin projection, $\beta \approx 0.65$ K the magnetic anisotropy constant, $g \approx 1.94$ the gyromagnetic factor, μ_B the Bohr magneton, and H_z the external magnetic field. The Hamiltonian determines the Zeeman energy release Q and the energy barrier E_a of the spin transition (in kelvin), see Fig. 1, which depend on the magnetic field as

$$E_a = \beta S^2 - g\mu_B H_z S + g^2\mu_B^2 H_z^2/4\beta, \quad (1)$$

$$Q = 2g\mu_B H_z S. \quad (2)$$

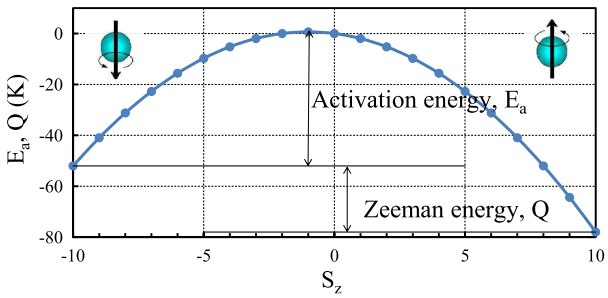

FIG. 1 (color online). The energy levels for the Mn_{12} molecule in the external field $H_z = 1$ T.

The energy barrier decreases with the field while the Zeeman energy increases linearly. Next, we consider a stationary magnetic detonation in a crystal of molecular magnets, which propagates with velocity D, sets crystal matter in motion with velocity u, and modifies its temperature T, pressure P, density ρ, and the fraction of molecules in the metastable state a. The values of u, T, P, ρ, and a vary within the detonation front. We adopt the reference frame of the detonation front and find the conservation laws of mass, momentum, and energy

$$\rho_0 D = \rho u, \tag{3}$$

$$P_0 + \rho_0 D^2 = P + \rho u^2, \tag{4}$$

$$\varepsilon_0 + \frac{P_0}{\rho_0} + \frac{1}{2}D^2 + Q = \varepsilon + \frac{P}{\rho} + \frac{1}{2}u^2 + Qa, \tag{5}$$

where ε is thermal energy per molecule. The label 0 designates matter ahead of the detonation front with $a_0 = 1$, $u_0 = D$. In the theory of shock waves one often introduces the volume per unit mass $V \equiv 1/\rho$; here we describe the matter compression by the scaled density ratio $r = \rho/\rho_0 = V_0/V$. The conservation laws Eqs. (3)–(5) have to be complemented by an equation of state. Following Ref. [15], we represent the pressure and energy of condensed matter at low temperature as a combination of elastic and thermal components as

$$P = \frac{c_0^2}{V_0 n}(r^n - 1) + \frac{A\Gamma k_B T^{\alpha+1} r}{(\alpha+1)V_0\Theta_D^\alpha}, \tag{6}$$

$$\varepsilon = \frac{c_0^2}{n}\left(\frac{r^{n-1}-1}{n-1} + \frac{1}{r} - 1\right) + \frac{Ak_B T^{\alpha+1}}{(\alpha+1)\Theta_D^\alpha}, \tag{7}$$

where the power exponent is $n \approx 4$ as suggested in [15], $\Gamma \approx 2$ is the Gruneisen coefficient, Θ_D is the Debye temperature with $\Theta_D = 38$ K for Mn_{12}, k_B is the Boltzmann constant, $A = 12\pi^4/5$ corresponds to the simple crystal model, $\alpha = 3$ is the problem dimension. Thus, Eqs. (3)–(7) provide a complete system for describing magnetic detonation in molecular magnets.

The properties of shocks (detonations) are represented by the Hugoniot (detonation) curves $P = P(V, a)$, which show all possible final states behind a shock (detonation) determined by Eqs. (3)–(7) for a given initial state and a specified energy release [14]. Any final state corresponds to a particular front speed D. We reduce Eqs. (3)–(7) to a single equation for the shock or detonation fronts as

$$\left(\frac{1}{\Gamma} - \frac{r-1}{2}\right)\frac{P}{\rho_0} = rQ(1-a) + \left(r + \frac{r-1}{2}\Gamma\right)\varepsilon_0 + \frac{c_0^2}{n-1}\left[r - 1 - \left(1 - \frac{n-1}{\Gamma}\right)\frac{r^n - 1}{n}\right]. \tag{8}$$

We stress that Eqs. (3)–(8), in general, hold for fronts with finite internal structure, though shock width is typically negligible in comparison with the total detonation width. In the case of zero energy release ($a_s = 1$), Eq. (8) describes the Hugoniot curve for a shock wave (label s). The leading shock compresses the sample, increases temperature, and hence facilitates the spin reversal with the Zeeman energy release, so that a changes from 1 to 0 within the detonation front. The released Zeeman energy provides expansion of the medium, which acts like a piston and supports the leading shock. In the case of the completed spin reversal ($a = 0$), Eq. (8) describes the final state behind the detonation front (label d). The inset of Fig. 2 shows the Hugoniot and detonation curves found using Eq. (8) for $H = 4$ T. We assume that there is no external atmospheric pressure and the initial temperature is negligible, which corresponds to the initial point ($V = V_0$; $r = 1$; $P = 0$). Because of the energy release, the detonation curve is always above the Hugoniot one. In the case of Mn_{12} we find that the elastic contribution to the pressure and energy dominates over the thermal one, which leads to a rather weak detonation with the shock and detonation curves almost coinciding as shown at the inset of Fig. 2. A self-supporting detonation corresponds to the Chapman-Jouguet (CJ) regime, for which velocity of the products in the reference frame of the front is equal to the local sound speed [14]. The CJ point at the detonation curve is determined by the tangent line connecting the initial state and the detonation curve. Since the detonation and Hugoniot curves are extremely close at the inset of Fig. 2, the intersection of the tangent line cannot be seen in the traditional representation of the curves. In order to make the figure illustrative, we subtract this tangent line from the Hugoniot and detonation curves in Fig. 2. In the

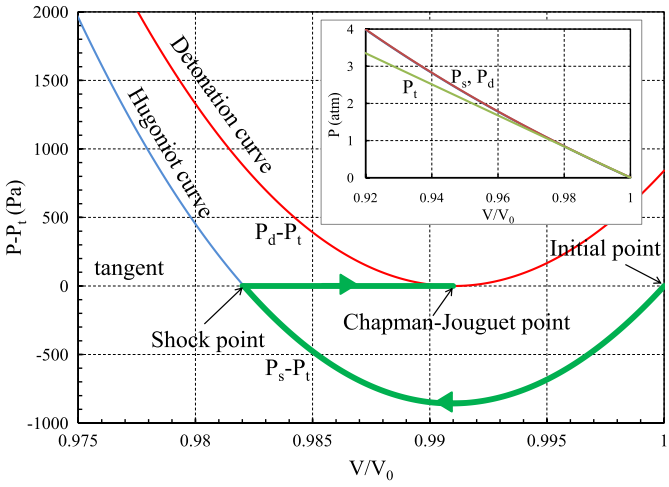

FIG. 2 (color online). The inset: Traditional presentation of the Hugoniot and detonation curves and the tangent line to the detonation curve in Mn_{12} acetate for the external magnetic field $H_z = 4$ T. The main plot: The Hugoniot and detonation curves with the tangent line extracted; label "t" stands for tangent.

new representation, the tangent line corresponds to the zero line, while the Hugoniot and detonation curves may be distinguished quite well. Changes of the crystal parameters in the CJ detonation are indicated by the bold line with arrows: the parabolic piece of the line shows modifications within the leading shock, while the straight piece describes the Zeeman energy release in the detonation behind the shock until the spin reversal is complete in the final CJ point. The density and the pressure acquire maximum values at the shock front and then decrease due to the energy release.

We notice from Fig. 2 that the Mn_{12} crystal is compressed by a few percent in the detonation wave, which makes an analytical theory for the detonation parameters possible using expansion $r = 1 + \delta$ with $\delta \ll 1$. Then, to the leading terms in δ, Eqs. (3)–(8) lead to

$$P = \rho_0[\Gamma Q(1 - a) + c_0^2\delta], \tag{9}$$

$$T^{\alpha+1} = (\alpha + 1)\frac{\Theta_D^\alpha}{Ak_B}\left[Q(1 - a) + \frac{n + 1}{12}c_0^2\delta^3\right]. \tag{10}$$

We find the final compression behind the detonation front as $\delta_d = c_0^{-1}\sqrt{2\Gamma Q/(n + 1)}$; the compression behind the leading shock is larger by a factor of 2, $\delta_s \approx 2\delta_d$. The detonation speed may be found from Eq. (3) as

$$D = c_0[1 + (n + 1)\delta_d/2] = c_0 + \sqrt{(n + 1)\Gamma Q/2}. \tag{11}$$

The second term in the right-hand side of Eq. (11) is less than 2% when the magnetic field is smaller than 4 T, so that this correction is beyond the accuracy of the present experiments on magnetic avalanches. Then the numerical value of the detonation speed may be taken approximately equal to the sound speed ($D \approx 2000$ m/s), being almost independent of the magnetic field. Substituting $\delta = \delta_s$, $a_s = 1$, and $\delta = \delta_d$, $a_d = 0$ into Eqs. (9) and (10), we find the analytical formulas for pressure and temperature at the shock and behind the detonation front, respectively. Taking into account Eq. (2), these formulas specify the dependence of the detonation parameters on the external magnetic field. The maximum value of shock pressure is below 1.2 atm for 10 T. Thus, due to the small compression and the moderate pressure increase, the magnetic detonation does not destroy the magnetic properties of the crystals, which is extremely important for the studies of molecular nanomagnets. For the combustion science, the obtained results provide also a unique example of an extremely weak detonation. Figure 3 demonstrates excellent agreement of the analytical theory and the numerical solution to Eq. (8) for density and temperature at the shock wave and behind the detonation front. The crystal temperature increases considerably because of the shock, which stimulates a fast spin reversal and a further temperature increase. The temperature at the shock is comparable to that expected for the magnetic deflagration [6–9], which also makes the reaction time comparable in both processes.

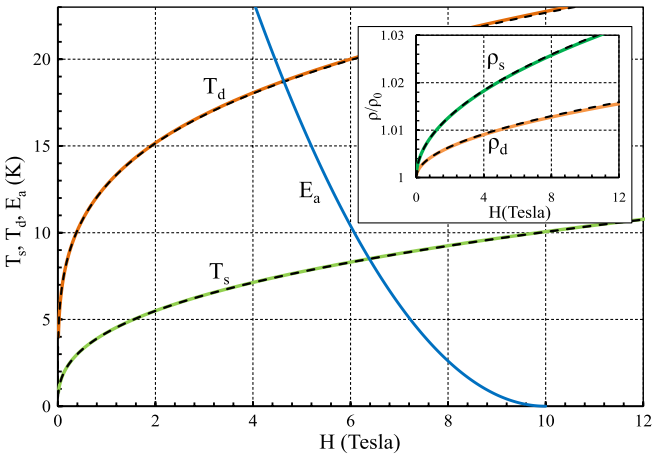

FIG. 3 (color online). Temperature and density at the leading shock and behind the detonation front versus the external magnetic field. Solid lines show exact numerical solution; the dashed lines stand for the analytical theory.

In combustion, the temperature at the leading shock in the detonation wave is quite small in comparison with the activation energy of the chemical reactions, so that the active reaction zone lags considerably behind the shock [14]. The situation may be quite different in magnetic detonation. When the magnetic field is stronger than 2–3 T, the shock temperature is relatively high ($E_a/T_s < 5$) so that active spin reversal starts right at the shock wave. Figure 3 presents also the energy barrier, which decreases with the magnetic field and vanishes for $H > 10$ T. Then the metastable state turns unstable, and the molecules may settle down freely to the ground state. Hence one may interpret magnetic avalanches as detonation or deflagration only for $H < 10$ T.

Finally, we describe the internal structure of the magnetic detonation front. In the reference frame of the moving front, the molecule fraction with the spin opposite to the field direction is determined by [10]

$$u\partial_x a = (a/\tau_R)\exp(-E_a/T), \tag{12}$$

where $\tau_R \sim 10^{-7}$ s is a constant of time dimension characterizing the spin reversal [6–9]. We integrated Eq. (12) numerically together with Eqs. (3) and (6) along the tangent line in Fig. 2, from the shock to the CJ point; the obtained profiles are depicted in Fig. 4 for $H = 3$ T. The background shading represents the energy release due to the spin reversal; the temperature and the pressure are scaled to their maximal values. The coordinate is scaled by the characteristic length $L_0 \equiv c_0\tau_R \sim 0.2$ mm; using this value we can estimate the characteristic width of the stationary detonation front to a few mm. The applied magnetic field influences strongly the reaction rate and thus the front width. For magnetic fields higher than 5 T, the detonation width is <1 mm, while for a weaker field the width may increase considerably. For this reason, the

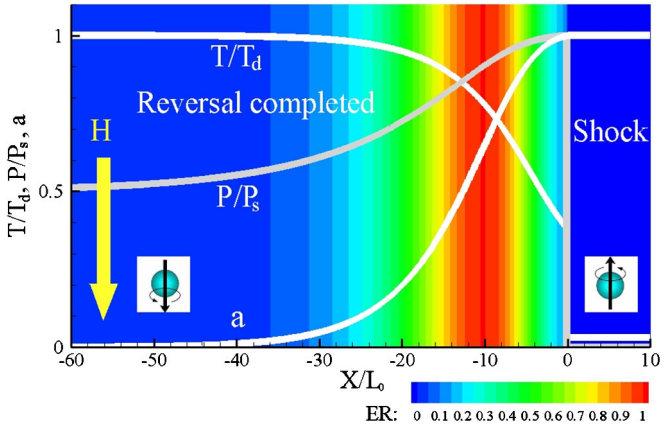

FIG. 4 (color online). Stationary profiles of the scaled temperature, pressure, and fraction of molecules in the metastable state for $H_z = 3$ T. The background shading shows the energy release scaled by the maximal value.

stationary detonation in molecular magnets may only be observed in experiments using high enough magnetic fields or the resonant field as in Ref. [13], which imply a strong decrease of the activation energy, reaction time and the front width. The typical scales in Ref. [13] were about a few mm, so that the fast avalanche regime observed experimentally was, presumably, a nonstationary detonation in the process of development. This conclusion explains rather long duration of the observed induction peaks (spin reversal), ~ 50 μs, in Fig. 2 of Ref. [13], in comparison with the time of front propagation in a sample, ~ 1 μs. This explains also dependence of the average avalanche speed on the magnetic sweep rate in Ref. [13]. Though our theory demonstrates stationary detonation speed almost independent of the magnetic field, $D \approx c_0$, the time of detonation ignition in the cases of both direct and indirect triggering depends on the energy implosion rate [14,16], i.e., the sweep rate. At high implosion rates detonation may be triggered faster and the experimentally observed average avalanche speed increases. At low rates the triggering process is slower, the average front speed decreases and the sample size may be too small for detonation triggering. Still, the experimental information on the fast magnetic avalanches is too limited and too uncertain at present to make any definite conclusion about the unsteady detonation development. This process may happen in the form of direct ignition by straightforward energy deposition, or indirect ignition through deflagration-to-detonation transition [14,16]. For example, spin reversal close to the resonant magnetic field in Ref. [13] implies an abrupt decrease of the activation energy E_a and a fast acceleration of the deflagration front. An accelerating deflagration pushes a shock, which may trigger the detonation [16]. Within the experimental data of Ref. [13], one may also discuss the possibilities of underdeveloped, decelerating, and dying detonation [14], and other options like radiative coupling between the molecular clusters [13]. To select one of these options, refined experiments are required, able to trace time evolution of the avalanche front with high-accuracy measurements of the instant front speed, not only the average speed.

To summarize, in this Letter we have demonstrated the possibility of magnetic detonation in molecular magnets, which explains the ultrafast spin avalanches presented in Ref. [13]. The detonation propagates with a velocity slightly higher than the sound speed, i.e., 3 orders of magnitude faster than the magnetic deflagration observed before [6–9]. We have shown that crystal heating by the leading shock triggers the spin reversal in the magnetic detonation. In contrast to traditional detonations in combustion, characterized by strongly supersonic velocities and destructively high pressure, magnetic detonations involve moderate pressure increase, below 1 atm even for considerable magnetic fields. Thus, magnetic detonation does not destroy the magnetic properties of the crystals, a very important conclusion in view of possible applications of molecular magnets to, e.g., quantum computing.

This work was supported by the Swedish Research Council and by the Kempe Foundation. The authors thank Petter Minnhagen, Bertil Sundqvist, Thomas Wågberg, Sune Pettersson, Tatiana Makarova, and Valeria Zagainova for useful discussions.

[1] D. Gatteschi and R. Sessoli, Angew. Chem., Int. Ed. **42**, 268 (2003).
[2] E. del Barco, A. D. Kent, S. Hill, J. M. North, N. S. Dalal, E. Rumberger, D. N. Hendrikson, N. Chakov, and G Christou, J. Low Temp. Phys. **140**, 119 (2005).
[3] R. Sessoli, D. Gatteschi, A. Caneschi, and M. A. Novak, Nature (London) **365**, 141 (1993).
[4] J. R. Friedman, M. P. Sarachik, J. Tejada, and R. Ziolo, Phys. Rev. Lett. **76**, 3830 (1996).
[5] L. Thomas, F. Lionti, R. Ballou, D. Gatteschi, R. Sessoli, and B. Barbara, Nature (London) **383**, 145 (1996).
[6] Y. Suzuki, M. P. Sarachik, E. M. Chudnovsky, S. McHugh, R. Gonzalez-Rubio, N. Avraham, Y. Myasoedov, E. Zeldov, H. Shtrikman, N. E. Chakov, and G. Christou, Phys. Rev. Lett. **95**, 147201 (2005).
[7] A. Hernandez-Minguez, J. M. Hernandez, F. Macia, A. Garcia-Santiago, J. Tejada, and P. V. Santos, Phys. Rev. Lett. **95**, 217205 (2005).
[8] S. McHugh, R. Jaafar, M. P. Sarachik, Y. Myasoedov, A. Finkler, H. Shtrikman, E. Zeldov, R. Bagai, and G. Christou, Phys. Rev. B **76**, 172410 (2007).
[9] A. Hernandez-Minguez, F. Macia, J. M. Hernandez, J. Tejada, and P. V. Santos, J. Magn. Magn. Mater. **320**, 1457 (2008).
[10] D. A. Garanin and E. M. Chudnovsky, Phys. Rev. B **76**, 054410 (2007).
[11] D. Villuendas, D. Gheorghe, A. Hernandez-Minguez, F. Macia, J. M. Hernandez, J. Tejada, R. J. Wijngaarden, Europhys. Lett. **84**, 67010 (2008).

[12] M. Modestov, V. Bychkov, and M. Marklund, Phys. Rev. B **83**, 214417 (2011).

[13] W. Decelle, J. Vanacken, V. V. Moshchalkov, J. Tejada, J. M. Hernandez, and F. Macia, Phys. Rev. Lett. **102**, 027203 (2009).

[14] C. K. Law, *Combustion Physics* (Cambridge University Press, New York, 2006).

[15] Ya. B. Zeldovich and Yu. P. Raizer, *Physics of Shock Wave and High-Temperature Hydrodynamic Phenomena* (Dover Publications, Inc., Mineola, NY, 2002).

[16] V. Bychkov and V. Akkerman, Phys. Rev. E **73**, 066305 (2006); V. Akkerman, C. K. Law, and V. Bychkov, Phys. Rev. E **83**, 026305 (2011).